

# On the $\eta$ and $f_1(1420)$ Couplings to the Nucleon

S. Neumeier<sup>1</sup> and M. Kirchbach<sup>2,3</sup>

<sup>1</sup>*Institut für Theoretische Physik, Universität Leipzig, D-04109 Leipzig, Germany*

<sup>2</sup>*Institut für Kernphysik, Universität Mainz, D-55099 Mainz, Germany*

<sup>3</sup>*Escuela de Física de la UAZ, AP C-600, Zacatecas, ZAC 98068 Mexico*

We consider neutral pseudoscalar,  $\eta$ , and axial vector,  $f_1(1420)$ , mesons in the OZI-rule-respecting flavor basis,  $\{(\bar{s}s), \frac{1}{\sqrt{2}}(\bar{u}u + \bar{d}d)\}$ , and suggest a scenario for their coupling to the nucleon. Within this framework, the non-strange parts of the  $\eta N$  and  $f_1 N$  couplings are modeled by means of triangular  $a_0 \pi N$ , and  $KK^*(\Lambda/\Sigma)$  vertices, while the strange ones partly proceed via Goldberger-Treiman relations, which have been concluded solely on the grounds of current universality. The suggested model explains the observed suppression of the  $\eta N$  coupling with respect to the constituent quark model expectations, and predicts the coupling of  $f_1$  to the nucleon.

## I. INTRODUCTION

The present paper devotes itself to the study of couplings of neutral pseudoscalar and axial vector mesons, such as  $\eta$  and  $f_1(1420)$ , to the nucleon in the OZI-rule-respecting flavor basis:  $\{(\bar{s}s), \frac{1}{\sqrt{2}}(\bar{u}u + \bar{d}d)\}$ . In the process, the surprising smallness of the  $\eta N$  coupling observed in various reactions finds a natural explanation. This problem has recently been reviewed in Ref. [1].

In the considered framework, the  $(\bar{s}s)$  components of the  $\eta$  and  $f_1(1420)$  wave functions, couple to the nucleon partly at tree-level via a Goldberger-Treiman (GT) relation that follows from the universality of the strange axial quark current, and partly via the gluon axial current. On the contrary, within the context of current universality, tree-level  $\frac{1}{\sqrt{2}}(\bar{u}u + \bar{d}d)N$  couplings are ruled out as the weak axial current does not contain the light flavors in a symmetric combination [1]. We here take a pragmatic position and mimic such vertices by means of triangular corrections. To be specific, we first bridge the initial  $\frac{1}{\sqrt{2}}(\bar{u}u + \bar{d}d)$  quarkonium to the meson cloud surrounding the nucleon and then couple the secondary mesons to universal currents. For example, the  $\frac{1}{\sqrt{2}}(\bar{u}u + \bar{d}d)$  part of the  $\eta$  wave function (to be denoted by  $\eta^q$ ) can be linked to the charged nucleon vector and axial vector currents by means of  $a_0 \pi N$  triangular vertices. Indeed, the  $a_0$  meson picks up the isotriplet vector current, while  $\pi$  selects the isotriplet axial one. In other words, we approximate  $\langle \eta^q N | J_{\mu,5}^q | N \rangle$  by  $\langle \eta \pi | a_0 \rangle \langle a_0 N | N \rangle \langle N \pi | N \rangle$ . Similarly, the  $\frac{1}{\sqrt{2}}(\bar{u}u + \bar{d}d)$  part from the  $f_1$  state (to be denoted by  $f_1^q$ ) is coupled to the nucleon by means of  $KK^*(892)(\Lambda/\Sigma)$  triangles. In due course, the couplings of the neutral pseudoscalar and axial vector mesons to the nucleon arise as combinations of the small fraction of nucleon helicity carried by the strange quark sea, and the small triangular vertex corrections. It is not surprising, therefore, that  $g_{\eta NN}$  appears suppressed relative to quark model predictions based on the octet Goldberger-Treiman relation. In this way, instead of interpreting the smallness of the  $\eta N$  coupling in terms of a suppressed nucleon octet axial matrix element<sup>1</sup>, we here rather reformulate this problem in terms of an enhancement of axial  $(\bar{s}s)N$  couplings due to vertex corrections.

A method similar in spirit to the one presented here but of different techniques is the so-called meson cloud model of Ref. [2]. There, the authors study the influence of the mesons surrounding the nucleon on its electromagnetic and weak vector form factors in terms of a nucleon wave function having a non-negligible overlap with the nucleon-meson scattering continuum. We here focus rather on the isoscalar axial form factor.

The paper is organized as follows. In the next section we briefly outline the calculation scheme of  $\eta NN$  and  $f_1(1420)NN$  vertices in the flavor-basis. In Sect. 3 the effective  $\eta NN$  vertex is calculated from the  $\pi a_0(980)N$  triangular vertex, while Sect. 4 contains the results on the effective  $f_1(1420)$  meson nucleon-couplings associated with the  $KK^*(892)Y$  triangle. The paper ends with a short summary.

---

<sup>1</sup>Note, that the problem of the suppression of the axial octet-nucleon coupling has been addressed in Ref. [3] within the framework of SU(6) chiral perturbation theory to one-loop order. There, the strong dependence of the result on the  $N$ - $\Delta$  mass splitting was revealed and the necessity for higher-order corrections discussed.

## II. THE $\eta(\mathbf{F}_1)N$ COUPLING IN THE FLAVOR BASIS

The  $\eta$  wave function in the  $\{(\bar{s}s), \frac{1}{\sqrt{2}}(\bar{u}u + \bar{d}d)\}$  flavor basis is parametrized as [4]:

$$\begin{aligned} |\eta\rangle &= \cos\theta |\eta^q\rangle - \sin\theta |\eta^s\rangle, \\ \cos\theta &= 0.773, \quad \sin\theta = 0.634, \\ \eta^q &= \frac{1}{\sqrt{2}}(\bar{u}u + \bar{d}d), \quad \eta^s = \bar{s}s. \end{aligned} \quad (1)$$

In the following we assume the pseudoscalar  $\eta(\eta')N$  coupling  $g_{\eta(\eta')NN}$  to be patterned after the states flavor mixing

$$g_{\eta NN} = g_{\eta^q NN} \cos\theta - g_{\eta^s NN} \sin\theta, \quad (2)$$

$$g_{\eta' NN} = g_{\eta^q NN} \sin\theta + g_{\eta^s NN} \cos\theta, \quad (3)$$

In order to obtain  $g_{\eta^s NN}$ , the pseudoscalar coupling of the  $0^-$  strange quarkonium to the nucleon, one may exploit Sakurai's idea on current universality and field-current identity to relate the tree-level part of  $g_{\eta^s NN}$  to the weak decay constant  $f_{\eta^s}$  via a Goldberger-Treiman type relation

$$g_{\eta^s NN}^{GT} = \frac{g_A^s}{f_{\eta^s}} m_N. \quad (4)$$

Here,  $m_N$  and  $g_A^s$  are in turn the nucleon mass and the strange axial coupling. The GT-relation in Eq. (4) can be interpreted as a consequence of  $(\bar{s}s)$ -pole dominance of the strange quark axial current (see Fig. 1). The net  $\eta N$  coupling contains in addition a term, here denoted by  $g_{\eta^s NN}^R$ , and which is associated with the pseudoscalar  $\eta^s(\tilde{G})$  coupling,

$$\mathcal{V}_{\eta^s NN}^R = g_{\eta^s NN}^R m_{\eta'}^2 f_{\pi^0} \bar{U}_N(\vec{p}') \tilde{G} G \mathcal{U}_N(\vec{p}) \phi_{\bar{s}s}. \quad (5)$$

Here,  $\mathcal{U}_N(\vec{p})$  is the nucleon Dirac spinor,  $G$  is the gluon field,  $\tilde{G}$  is its dual,  $\phi_{\bar{s}s}$  denotes the strange quarkonium field. The  $\eta'$  mass  $m_{\eta'}$  and the pion weak decay constant  $f_{\pi^0}$  serve as scale parameters. In other words,  $g_{\eta NN}$  decomposes into

$$g_{\eta^s NN} = g_{\eta^s NN}^{GT} - g_{\eta^s NN}^R, \quad (6)$$

A rough estimate for  $g_{\eta^s NN}^R$  can be obtained from Shore-Venziano's expression [5] for  $g_{\eta' NN}$ , the pseudoscalar  $\eta'N$  coupling,

$$g_{\eta' NN} = g_{\eta' NN}^{GT} - g_{\eta' NN}^R. \quad (7)$$

Here,  $g_{\eta' NN}^R = \frac{1}{\sqrt{3}} f_{\pi^0} m_{\eta'}^2 g_{GNN}$ , with  $g_{GNN}$  standing for the  $(\tilde{G}G)N$  coupling. With the numerical values for  $g_{\eta' NN} \approx 1$ , and  $g_{\eta' NN}^{GT} = 1.67$  deduced from [6] after accounting for the additional factor of  $1/\sqrt{2}$  in their current normalizations, we obtain  $g_{\eta' NN}^R \approx 0.67$ . In noticing that

$$\sqrt{3} g_{\eta' NN}^R = g_{(\bar{u}u) NN}^R + g_{(\bar{d}d) NN}^R + g_{(\bar{s}s) NN}^R \quad (8)$$

and assuming  $g_{(\bar{q}_i q_i) NN}^R$  to be flavor independent, we estimate  $g_{\eta^s NN}^R \approx 0.4$ .

On the other hands, the strange axial coupling  $g_A^s$  that enters the strange GT relation equals  $\Delta s$ , the genuine quark part of  $a_s$ , the fraction of nucleon polarization carried by the strange quark-gluon sea. In the notation of Ref. [7]  $a_s$  is given by

$$a_s(Q^2) = \Delta s - \frac{\alpha_s(Q^2)}{2\pi} \Delta g(Q^2). \quad (9)$$

In using the values of  $a_s(10 \text{ GeV}^2) = -0.10 \pm 0.02$ ,  $\alpha_s(10 \text{ GeV}^2) = 0.25$ , and  $\Delta g(10 \text{ GeV}^2) = 2 \pm 1.3$  from Ref. [7], one finds  $\Delta s = -0.02$ . We will consider this value as compatible with zero. In the following,  $g_{\eta^s NN}^{GT}$  will be neglected, so that

$$g_{\eta^s NN} \approx -g_{\eta^s NN}^R \approx -0.4. \quad (10)$$

This is the quantity that we will keep in Eq. (2)

In general, pseudoscalar meson-nucleon couplings,  $g_{MNN}$ , are related to gradient couplings,  $f_{MNN}$ , via the well known equality [10]

$$\frac{g_{MNN}}{2m_N} = \frac{f_{MNN}}{m_M}, \quad (11)$$

with  $m_M$  standing for the meson mass. That the GT-relation from Eq. (4) entirely originates from (strange) axial current universality is expressed by means of the following current-current couplings:

$$\begin{aligned} \mathcal{V}_{\eta^s NN}^s &= \frac{1}{f_{\eta^s}^2} J^{s(N)} \cdot J^{(\eta^s)} = \frac{1}{f_{\eta^s}^2} g_A^s(Q^2) \bar{U}_N(p') \gamma \gamma_5 \frac{\mathbb{1}}{2} U_N(p) \cdot f_{\eta^s} i q \phi_{\eta^s}, \\ \mathcal{V}_{f_1^s NN}^s &= \frac{1}{m_{f_1^s}^2} J^{s(N)} \cdot J^{(f_1^s)} = \frac{1}{m_{f_1^s}^2} g_A^s(Q^2) \bar{U}_N(p') \gamma \gamma_5 \frac{\mathbb{1}}{2} U_N(p) \cdot f_{f_1^s} m_{f_1^s}^2 \phi_{f_1^s}. \end{aligned} \quad (12)$$

Here,  $\phi_{\eta^s}$  and  $\phi_{f_1^s}$  are the respective  $\bar{s}s$  parts of the  $f_1$  and  $\eta$  fields, while  $J^{\eta^s}$  and  $J^{f_1^s}$  are the associated axial currents. The combination  $g_A^s f_{f_1^s}/2$  is identified with the  $f_1^s(1420)N$  contact coupling  $f_{f_1^s NN}^s$ , while  $g_A^s/2f_{\eta^s}$  is associated with the gradient  $\eta^s N$  coupling, i.e. one defines

$$\frac{f_{\eta^s NN}^s}{m_{\eta^s}} = \frac{g_A^s}{2f_{\eta^s}}, \quad f_{f_1^s NN}^s = \frac{g_A^s f_{f_1^s}}{2}, \quad \text{with } g_A^s = \Delta s. \quad (13)$$

Indeed, Eq. (4) is reproduced in inserting the first of Eqs. (13) into (11).

As long as at tree level the contact  $\eta N$  coupling appears proportional to  $\Delta s$  rather than follows the octet GT-relation  $f_{\eta s NN}/m_{\eta s} = g_A^s/(2f_{\eta s})$  of Ref. [11], the  $\eta$  meson can be interpreted as a “partial” strange Goldstone boson, a result already conjectured in a previous work [1]. Note, that the accuracy of GT-relations has been reliably proven only for the case of the pion-nucleon system [12]. The subtle reason for this situation can be understood if we note that mesons transporting weak interaction are not same as such participating strong interaction. This is due to the fact that the electroweak gauge group  $SU(2)_L \otimes U(1)$  and the strong flavor group  $SU(3)_F$  do not share, in general, common multiplets. Because of that, the weak interaction is incapable to recognize the  $\eta$  meson as a particle different but a strange quarkonium. The mismatch between the flavor contents of strong and electroweak spin-0 mesons has been studied extensively, for example, in Ref. [13] by means of F-spin breaking through the electroweak gauge symmetry. Using the genuine electroweak meson states from [13] in the construction of weak nucleon-nucleon potentials is an interesting goal for future research as it might modify interpretation of parity violation effects in nuclei. Now, due to the smallness of  $\Delta s$ , the  $\eta$  and  $f_1(1420)$  mesons practically decouple at tree level from the nucleon. This might be one of the main reasons for which a strong suppression of the  $\eta N$  couplings has frequently been found over the years by various data analyses of  $\eta$  photo-production off proton at threshold [14], as well as nucleon-nucleon (NN) and nucleon-hyperon (NY) phase shifts [15]. Same observation applies to  $f_{f_1^s}$ . In the following, the strange tree level couplings will be of minor importance and neglected.

Compared to  $g_{\eta s NN}$ , the calculation of the pseudoscalar  $\eta^q NN$  coupling can not be discussed in terms of universality of the non-strange isosinglet axial current, as the weak axial current does not contain the light flavors in a symmetric combination. Therefore, no obvious GT-relation can be written for  $g_{\eta^q NN}$  (see Fig. 2).

In the following two sections we consider the  $\eta^q NN$  and  $f_1^q NN$  vertices to proceed entirely via small but non-negligible triangular loops of the type  $a_0 \pi N$  in Fig. 4, and  $KK^*(\Lambda/\Sigma)$  in Fig. 7, respectively.

### III. EFFECTIVE $\eta NN$ VERTICES

In this section we calculate the gradient and pseudoscalar coupling constants of the  $\eta$  meson to the nucleon by means of triangular vertices involving the  $a_0(980)$  and  $\pi$  mesons.

The special role of the  $a_0(980)\pi N$  triangular diagram as the dominant one-loop mechanism for the  $\eta N$  coupling is emphasized by the circumstance that the  $a_0(980)$  meson is the lightest meson with a two particle decay channel containing the  $\eta$  particle [9].

The contributions of heavier mesons such as the isotriplet  $a_2(1320)$  tensor meson with an  $\eta\pi$  decay channel and the isoscalar  $f_0(1400)$ ,  $f_2'(1525)$  and  $f_2(1720)$  tensor mesons with  $\eta\eta$  decay channels will be left out of consideration because of the short range character of the corresponding triangle diagrams on the one side,<sup>2</sup> and because of the

---

<sup>2</sup>The same argument applies to the neglect of the  $f_0(1590)\eta N$  triangular vertex.

comparatively small couplings of the tensor mesons to the nucleon [17,18] on the other side. The  $\pi a_0 N$  triangular couplings in (Fig. 3) have been calculated using the following effective Lagrangians:

$$\mathcal{L}_{a_0\eta\pi}(x) = f_{a_0\eta\pi} \frac{m_{a_0}^2 - m_\eta^2}{m_\pi} \phi_\eta^\dagger(x) \vec{\phi}_\pi(x) \cdot \vec{\phi}_{a_0}(x) \quad (14)$$

$$\mathcal{L}_{\pi NN}(x) = \frac{f_{\pi NN}}{m_\pi} \bar{N}(x) \gamma_\mu \gamma_5 \vec{\tau} N(x) \cdot \partial^\mu \vec{\phi}_\pi(x), \quad (15)$$

$$\mathcal{L}_{a_0 NN}(x) = g_{a_0 NN} i \bar{N}(x) \vec{\tau} N(x) \cdot \vec{\phi}_{a_0}(x). \quad (16)$$

Here  $f_{\pi NN}$  and  $g_{a_0 NN}$  in turn denote the pseudovector  $\pi N$  and the scalar  $a_0 N$  coupling constants. We adopt for  $f_{\pi NN}$  the standard value  $f_{\pi NN}^2/4\pi = 0.075$  and fit  $g_{a_0 NN}$  to data. The value of  $f_{a_0\eta\pi} = 0.44$  has been extracted from the experimental decay width [9] when ascribing the total  $a_0$  width to the  $a_0 \rightarrow \eta + \pi$  decay channel. Note that  $\mathcal{L}_{a_0\eta\pi}$  represents only a part of the full chiral Lagrangians of the  $a_0\eta\pi$  system constructed in Ref. [16]. The term containing the gradient  $\eta\pi$  coupling has not been taken into account so far as we restrict ourself to Lagrangians containing a minimal number of derivatives to ensure convergence of the expressions. Nonetheless, through the use of a gradient  $\pi N$  coupling, the triangular  $\eta NN$  vertex vanishes in the chiral limit despite the fact that the  $a_0\pi\eta$  vertex does not. In the following we will identify the nucleon Born term  $\langle \pi N | N \rangle \langle N | a_0 N \rangle$  entering the diagram in Fig. 4 with the full amplitude  $T_{\eta N}(\pi + N \rightarrow a_0 + N)$ , and parameterize it in terms of the following complete set of invariants

$$T_{\eta N}(\pi + N \rightarrow a_0 + N) = \bar{\mathcal{U}}_N(\vec{p}') \left( \frac{G_1(k^2)}{m_\eta} \not{k} \gamma_5 + G_2(k^2) \gamma_5 \right) \mathcal{U}_N(\vec{p}), \quad (17)$$

where the invariant functions  $G_1(k^2)$  and  $G_2(k^2)$  in turn correspond to pseudovector (PV) and pseudoscalar (PS) types of the  $\eta N$  coupling. Expressions for  $G_1(k^2)$  and  $G_2(k^2)$  can be found in evaluating the diagrams in Fig. 4 in accordance with the standard Feynman rules. We here systematically consider the incoming proton to be on its mass shell and make use of the Dirac equation, so that

$$\gamma_5 \not{p} \mathcal{U}_N(\vec{p}) = m_N \gamma_5 \mathcal{U}_N(\vec{p}), \quad (18)$$

holds. On the contrary, the outgoing proton has been considered to be off its mass shell with

$$\gamma_5 \not{p}' \mathcal{U}_N(\vec{p}) = \gamma_5 (\not{p} + \not{k}) \mathcal{U}_N(\vec{p}) = m_N \gamma_5 \mathcal{U}_N(\vec{p}) + \gamma_5 \not{k} \mathcal{U}_N(\vec{p}). \quad (19)$$

The final result on  $G_1(k^2)$  obtained in this way reads:

$$\begin{aligned} G_1(k^2) &= C \int_0^1 \int_0^1 dy dx \frac{c_1(x, y, k^2)}{\mathcal{Z}(m_N, m_\pi, m_{a_0}, x, y, k^2)}, \\ c_1(x, y, k^2) &= -\frac{1}{2} x(1-y) m_N m_\eta, \\ C &= \frac{3}{8\pi^2} \frac{m_{a_0}^2 - m_\eta^2}{m_\pi^2} f_{\pi NN} f_{a_0\eta\pi} g_{a_0 NN}. \end{aligned} \quad (20)$$

The corresponding expression for  $G_2(k^2)$  reads

$$\begin{aligned} G_2(k^2) &= C \int_0^1 \int_0^1 dy dx \frac{c_2(x, y, k^2)}{\mathcal{Z}(m_N, m_\pi, m_{a_0}, x, y, k^2)}, \\ c_2(x, y, k^2) &= -x(1-y) m_N^2. \end{aligned} \quad (21)$$

The function  $\mathcal{Z}(m_B, m_1, m_2, x, y, k^2)$  appearing in the last two expressions is defined as

$$\begin{aligned} \mathcal{Z}(m_B, m_1, m_2, x, y, k^2) &= m_N^2 x^2 (1-y)^2 + x^2 y k^2 + m_1^2 (1-x) + (m_2^2 - k^2) x y \\ &\quad + (m_B^2 - m_N^2) x (1-y). \end{aligned} \quad (22)$$

The remarkable feature of the analytical expressions for the pseudoscalar and pseudovector  $\eta N$  couplings is that they are given by *completely convergent* integrals and depend only on the  $a_0 \rightarrow \pi + \eta$  decay constant and the respective pion and  $a_0$  meson-nucleon couplings. The sources of uncertainty in the parameterization of the effective  $\eta NN$  vertex by means of the triangular  $a_0(980)\pi N$  diagram are associated with the  $a_0(980)N$  coupling constant and the  $\Gamma(\eta\pi)/\Gamma_{a_0}^{\text{tot}}$

branching ratio. For example, the coupling constant  $g_{a_0 NN}$  varies between  $\approx 3.11$  and  $\approx 10$  depending on the  $NN$  potential model version [17,18]. Because of that we give below the values for the gradient and pseudoscalar  $\eta N$  couplings following from the  $a_0\pi N$  triangular  $\eta N$  vertex as a function of the  $a_0 N$  coupling constant:

$$|G_1(k^2 = m_\eta^2)| = 0.06 g_{a_0 NN}, \quad |G_2(k^2 = m_\eta^2)| = 0.22 g_{a_0 NN}. \quad (23)$$

There are the quantities in Eqs. (20) and (21) which we shall interpret as the *effective* pseudovector and pseudoscalar  $\eta^q N$  coupling constants, respectively,

$$\cos \theta f_{\eta^q NN}^{\text{eff}}(k^2) = G_1(k^2), \quad \cos \theta g_{\eta^q NN}^{\text{eff}}(k^2) = G_2(k^2), \quad k^2 = m_\eta^2. \quad (24)$$

In combining the last equation with (2), and (10), one finds the following expression for the  $\eta N$  coupling:

$$g_{\eta NN} = 0.22 g_{a_0 NN} + 0.63 g_{\eta^s NN}^R \approx 0.22 g_{a_0 NN} + 0.25. \quad (25)$$

In using four different values for  $g_{a_0 NN}^2/4\pi$  reported in [17], [18], we calculate  $g_{\eta NN}^2/4\pi$  in Table 1. Our analyses suggest for the pseudoscalar  $\eta N$  coupling small but non-vanishing values. In comparing our predictions to data, we rely upon Refs. [14]. There, Tiator *et al.* interpreted the high-precision MAMI measurement of the differential cross sections in  $\eta$  photo-production off-proton near threshold in terms of the strongly suppressed  $g_{\eta NN}$  value of  $g_{\eta NN}^2/4\pi \approx 0.4$ . This result was concluded from the small  $P$  wave contribution to the almost flat angular distributions for a wide range of beam energies. Note, that a larger value for  $g_{\eta NN}$  has been extracted from total  $\bar{p}p$  cross sections in using dispersion relation techniques [19]. However, the latter procedure is endowed with more ambiguities than the straightforward calculation of the angular distributions from Feynman diagrams presented in Ref. [14].

From Eq. (17) one sees that the triangular  $a_0\pi N$  correction to the  $\eta NN$  vertex represents a mixture [20] of pseudovector (PV) and pseudoscalar (PS) types of  $\eta N$  couplings. This mixing is quite important for reproducing the form of the differential cross section for  $\eta$  photo-production off proton at threshold in Fig. 6. Note that such a mixing cannot take place for Goldstone bosons because their point-like gradient couplings to quarks are determined in a unique way. On the contrary, in case of extended effective meson-nucleon vertices, such a mixing can take place by means of Eq. (17). However, the PV-PS separation is model dependent and can not be interpreted as observable. Data compatibility with the PV-PS mixing created by the  $\pi a_0 N$  triangular correction to the  $\eta NN$  vertex is a further hint on the non-octet Goldstone boson nature of the  $\eta$  meson<sup>3</sup>. Finally, in estimating the  $\eta'$  nucleon coupling in terms of Eqs. (3), (10), (23), and (24) we find

$$g_{\eta' NN} = \frac{\sin \theta}{\cos \theta} 0.22 g_{a_0 NN} + \cos \theta g_{\eta^q NN}^R. \quad (26)$$

For the  $\eta$ - $\eta'$  mixing angle of  $\theta \approx 39.4^\circ$  and the maximal value of  $g_{a_0 NN} \approx 9.24$ , one finds  $g_{\eta' NN} \approx 1.41$  and in agreement with the estimate of Ref. [6]. Thus in simulating the anomalous  $\frac{1}{\sqrt{2}}(\bar{u}u + \bar{d}d)N$  coupling by the triangular  $a_0\pi N$  vertex we are able to explain the smallness of both the  $\eta' N$  and  $\eta N$  couplings.

---

<sup>3</sup>It should be noted that the analytical expressions for the  $\eta N$  couplings in Eqs. (21) and (20) differ from those obtained in [10] where the ambiguity in treating the off-shellness of the outgoing proton was not kept minimal.

TABLE I. The dependence of the  $\eta N$  coupling on  $g_{a_0 NN}$  following from Eq. (24)

$\frac{g_{a_0 NN}^2}{4\pi}$	0.77	1.075	3.71	6.79
$\frac{g_{\eta NN}^2}{4\pi}$	0.07	0.09	0.24	0.41

---

In the present calculation, the on-shell approximation  $p \cdot k = -p' \cdot k = -m_\eta^2/2$  was made only in evaluating the denominators of the Feynman diagrams, whereas in the nominators  $\not{p}'$  was consequently replaced by  $\not{p}' = \not{p} + \not{k}$ . In contrast to this, in [10] the above on-shell approximation was applied to the nominators too and, in addition, terms containing  $\not{p}'$  have been occasionally interpreted as independent couplings. Through the improper treatment of the off-shellness of the outgoing proton in [10], logarithmically divergent integrals have been artificially invoked in  $g_{\eta NN}$ .

#### IV. EFFECTIVE $F_1(1420)NN$ VERTICES

The internal structure of the axial vector meson  $f_1(1420)$  is still subject to some debates (see Note on  $f_1(1420)$  in [9]). Within the constituent quark model this meson is considered as the candidate for the axial meson ( $\bar{s}s$ ) state and therefore as the parity partner to  $\phi$  from the vector meson nonet. The basic difference between the neutral  $1^-$  and  $1^+$  vector mesons is that while the physical  $\omega$  and  $\phi$  mesons are almost perfect non-strange and strange quarkonia, respectively, their corresponding parity partners  $f_1(1285)$  and  $f_1(1420)$  are not. For these axial vector mesons strange and non-strange quarkonia appear mixed up by the angle  $\epsilon \approx 15^\circ$  (compare Ref. [21]):

$$|f_1(1285)\rangle = -\sin \epsilon (|\bar{s}s\rangle) + \cos \epsilon \frac{1}{\sqrt{2}}(|\bar{u}u + \bar{d}d\rangle), \quad (27)$$

$$|f_1(1420)\rangle = \cos \epsilon (|\bar{s}s\rangle) + \sin \epsilon \frac{1}{\sqrt{2}}(|\bar{u}u + \bar{d}d\rangle), \quad \epsilon \approx 15^\circ. \quad (28)$$

Therefore within this scheme the violation of the OZI rule for the neutral axial vector mesons appears quite different as compared to the pseudoscalar mesons. If one had to re-write the  $\eta$  wave function to the form of Eq. (28), one had to use  $\epsilon \approx (\frac{\pi}{2} + 39.3^\circ)$ . In general, as compared to pseudoscalar mesons, the axial vector meson sector respects better the OZI rule. This situation is often discussed in terms of significant glueball presence in the vector meson wave functions and as the consequence of the  $U(1)_A$  anomaly [22]. On the other side, the  $f_1(1420)$  meson seems alternatively to be equally well interpreted as a  $K^*\bar{K}$  molecule [23]. The coupling of this meson to the nucleon is not experimentally well established so far. The only information about it can be obtained from fitting  $NN$  phase shifts by means of generalized boson exchange potentials of the type considered in Refs. [17,18]. There, one finds that the coupling  $|g_{f_1 NN}| \approx 10$  to the nucleon of an effective  $f_1$  meson having same mass as the  $f_1(1285)$  meson is comparable to the  $\omega N$  coupling. Below we demonstrate that couplings of that magnitude can be associated to a large amount with triangular diagrams of the type  $KK^*Y$  with  $Y = \Lambda, \Sigma$ .

To calculate the  $KK^*Y$  triangular coupling in (Fig. 7) we use the following effective Lagrangians:

$$\mathcal{L}_{f_1 KK^*}(x) = f_{f_1 KK^*} \frac{m_{K^*}^2 - m_K^2}{m_K} K^\dagger(x) K^*(x)^\mu f_1(x)_\mu + h.c., \quad (29)$$

$$\mathcal{L}_{KYN}(x) = g_{KYN} i \bar{Y}(x) \gamma_5 N(x) K(x) + h.c., \quad (30)$$

$$\mathcal{L}_{K^*YN}(x) = -g_{K^*YN} \bar{N}(x) (\gamma^\mu K^*(x)_\mu + \frac{\kappa_V}{m_N + m_Y} \sigma^{\mu\nu} \partial_\nu K^*(x)_\mu) Y(x) + h.c. \quad (31)$$

Here,  $g_{KYN}$  stands for the pseudoscalar coupling of the kaon to the nucleon-hyperon ( $Y$ ) system,  $g_{K^*NY}$  denotes the vectorial  $K^*NY$  coupling,  $g_{K^*NY} \frac{\kappa_V}{m_N + m_Y}$  is the tensor coupling of the  $K^*$  meson to the baryon,  $K^*(x)_\mu$ , and  $f_1(x)_\mu$  in turn stand for the polarization vectors of the  $K^*$  and  $f_1$  mesons,  $K(x)$  is the kaon field, while  $N(x)$  and  $Y(x)$  are in turn the nucleon and hyperon fields.

A comment on the construction of the effective Lagrangian  $\mathcal{L}_{f_1 KK^*}$  is in place. Ogievetsky and Zupnik (OZ) [24] constructed a chirally invariant Lagrangian containing no more than two field derivatives to describe the dynamics of the  $a_1(1260)\rho(770)\pi$  system. Exploiting the fact that these mesons have the same external quantum numbers  $J^{PC}$  as the respective  $f_1(1420)$ ,  $K^*$ , and  $K$  mesons, the OZ Lagrangian might serve as a model for the  $f_1 K^* K$  system. However, the calculation shows up UV-divergent integrals which are to be maintained by additional cut-offs, i.e. by introducing form factors at both the  $KYN$ - and  $K^*YN$ -vertices [25]. This inconvenience makes the Lagrangian choice according to [24] less attractive than the present one given above by Eq. (29).

We adopt for the coupling constants the values implied by the Jülich potential [15]

$$\frac{g_{p\Lambda K^+}^2}{4\pi} = (-0.952)^2, \quad \frac{g_{p\Lambda K^*}^2}{4\pi} = (-1.588)^2, \quad \kappa_V = 4.5. \quad (32)$$

The value for  $f_{f_1 KK^*} = 1.97$  has been extracted from the experimental  $\Gamma_{\bar{K}K^*+h.c.}$  width of 17 MeV [9] and are compatible with the size of the corresponding GT relations for kaons. In identifying now the hyperon Born term  $\langle KY|Y\rangle\langle Y|K^*N\rangle$  entering the effective  $f_1 NN$  vertex with the full amplitude  $T_{f_1 N}(K + N \rightarrow K^* + N)$ , we expand the latter into the complete set of the following invariants

$$\begin{aligned} T_{f_1 N}(K + N \rightarrow K^* + N) = & \bar{U}_N(\vec{p}') \left( F_1(k^2) \gamma \cdot \epsilon_{f_1} \gamma_5 + \frac{F_2(k^2)}{m_{f_1}} \gamma \cdot \epsilon_{f_1} \gamma_5 \gamma \cdot k \right. \\ & \left. + \frac{F_3(k^2)}{m_N m_{f_1}} p \cdot \epsilon_{f_1} \gamma_5 \gamma \cdot k + \frac{F_4(k^2)}{m_N} p \cdot \epsilon_{f_1} \gamma_5 \right) U_N(\vec{p}). \end{aligned} \quad (33)$$

It will become clear in due course that the vector part of the  $K^*NY$  coupling contributes only to the  $F_2(k^2)$  and  $F_4(k^2)$  currents in Eq. (33). All the remaining terms are entirely due to the  $K^*NY$  tensor coupling. For small external momenta, i.e. when  $\not{p}'\mathcal{U}_N(\vec{p}) \approx m_N\mathcal{U}_N(\vec{p})$ , the number of the invariants reduces to three as the first term in Eq. (33) can be approximated by the following linear combinations of the  $F_2(k^2)$  and  $F_3(k^2)$  currents:

$$m_N\bar{\mathcal{U}}_N(\vec{p}')\gamma_5\not{k}\gamma_\mu\mathcal{U}_N(\vec{p}) = -p' \cdot k\bar{\mathcal{U}}_N(\vec{p})\gamma_5\gamma_\mu\mathcal{U}_N(\vec{p}) + p'_\mu\bar{\mathcal{U}}_N(\vec{p})\gamma_5\not{k}\mathcal{U}_N(\vec{p}). \quad (34)$$

One can make use of the approximation of Eq. (34) to estimate  $F_1(k^2)$ , the only invariant function which cannot be deduced in an unique way from the triangular  $KK^*Y$  diagrams because of the (logarithmically) divergent parts contained there.

The invariant functions  $F_i(k^2)$  are now evaluated by means of the diagrams of momentum-flow in Fig. 5 in using the techniques of the previous section. The various  $f_1N$  couplings can then be expressed in terms of the integrals

$$F_i(k^2) = \frac{1}{16\pi^2}f_{f_1KK^*}g_{KYNGK^*YN} \int_0^1 x dx \int_0^1 dy B_i(k^2). \quad (35)$$

The only divergent analytical expression is the one for  $B_1(k^2)$

$$\begin{aligned} B_1(k^2) &= 2\bar{\kappa} \frac{m_{f_1}^2 - m_{K^*}^2}{m_K} m_N (xm_Y - 2m_N) \frac{1}{Z} \\ &+ \bar{\kappa} k^2 \frac{m_{f_1}^2 - m_{K^*}^2}{m_K} (xy + (1-x)(8xy + x - 6)) \frac{1}{Z}, \\ &- 2\bar{\kappa} \frac{m_{f_1}^2 - m_{K^*}^2}{m_K} \ln \frac{\mathcal{Z}(m_Y, m_K, \Lambda_{K^*}, x, y, k^2) \mathcal{Z}(m_Y, \Lambda_K, m_{K^*}, x, y, k^2)}{\mathcal{Z}(m_Y, m_K, m_{K^*}, x, y, k^2) \mathcal{Z}(m_Y, \Lambda_K, \Lambda_{K^*}, x, y, k^2)}. \end{aligned} \quad (36)$$

All the remaining invariants are convergent and given below as

$$\begin{aligned} B_2(k^2) &= \frac{m_{f_1}^2 - m_{K^*}^2}{m_K} m_{f_1} [\bar{\kappa}(m_Y(-x^2y(1-y) + 3xy - 3x + 2) + xym_N) + (1-x(1+y))] \frac{1}{Z}, \\ B_3(k^2) &= -\bar{\kappa} m_{f_1} m_N \frac{m_{f_1}^2 - m_{K^*}^2}{m_K} ((1-y)(x^2(1+3y) - 3x) + 2) \frac{1}{Z}, \\ B_4(k^2) &= -2m_N \frac{m_{f_1}^2 - m_{K^*}^2}{m_K} [(x(1-y) - 1)(1 + \bar{\kappa} m_N x(1-y)) + \bar{\kappa} m_Y x(1+y)] \frac{1}{Z}, \\ Z &= \mathcal{Z}(m_Y, m_K, m_{K^*}, x, y, k^2). \end{aligned} \quad (37)$$

The numerical evaluation of the expressions in the last two equations leads to the following results:

$$\begin{aligned} F_1(k^2 = m_{f_1}^2) &= -8.56, & F_2(k^2 = m_{f_1}^2) &= 6.83, \\ F_3(k^2 = m_{f_1}^2) &= -3.77, & F_4(k^2 = m_{f_1}^2) &= -2.03, \\ m_{f_1} &= 1385.7 \text{ MeV}. \end{aligned} \quad (38)$$

In the spirit of Eqs. (2) and (28), we here identify  $F_1(m_{f_1}^2)$  with  $f_{f_1 NN} \sin \epsilon$ . These results show that all the couplings in Eq. (33) are noticeable and have to be taken into account in calculating  $\eta$  and  $f_1$  meson production cross sections. Note, however that recent analyses of data on electromagnetic strangeness production performed in [26] revealed a surprising suppression of the  $K^*YN$  vertices. Using the vertex constants from [26] would reduce the size of the  $f_1N$  couplings by at least an order of magnitude.

## V. SUMMARY

We developed a scenario for  $\eta NN$  and  $f_1 NN$  vertices, where the non-strange  $\frac{1}{\sqrt{2}}(\bar{u}u + \bar{d}d)$  quarkonia from the mesons wave functions were coupled to the nucleon by means of triangular vertex corrections, while the  $(\bar{s}s)N$  couplings were of Shore-Veneziano's type. We used phenomenological Lagrangians containing minimal number of derivatives to construct effective  $\eta N$  and  $f_1 N$  coupling strengths beyond the tree level in terms of triangular  $a_0\pi N$ , and  $KK^*(\Lambda/\Sigma)$  diagrams, respectively. We found all kinds of effective couplings (up to one) to be determined by divergenceless

expressions. Despite that the loop corrections dominate the tree-level ones, the net effect is a significant suppression of the couplings considered relative to quark model predictions. Remarkably, the  $\eta N$  and  $\eta' N$  couplings were found to be of comparable size, opposite to quark model predictions and in line with data. To be specific, the triangular  $a_0 \pi N$  vertex revealed itself as a successful effective mechanism for the  $\eta^q N$  coupling and led to a satisfactory explanation of the smallness of both  $g_{\eta NN}$  and  $g_{\eta' NN}$ .

### **Acknowledgements**

We wish to thank Hans J. Weber for continuous supportive discussions on the nature of the  $\eta N$  coupling mechanism, Martin Reuter for his interest and helpful remarks on particular group theoretical aspects, and Andreas Wirzba for his comments on the  $U(1)_A$  anomaly problems.

This work was partly supported by CONACYT, Mexico.



- 
- [1] M. Kirchbach and H.-J. Weber, Comm. Nucl. Part. Phys. **22**, 171 (1998).
  - [2] H. Holtman, A. Szczurek, and J. Speth, Nucl. Phys. **A596**, 631 (1996).
  - [3] M. J. Savage and J. Walden, Phys. Rev. **D55**, 5376 (1997).
  - [4] T. Feldmann, P. Kroll and B. Stech, Phys. Rev. **D58**, 114006 (1998).
  - [5] G. M. Shore and G. Veneziano, Phys. Lett. **B244**, 75 (1990); Nucl. Phys. **B381**, 23 (1992).
  - [6] T. Feldmann, Int. J. Mod. Phys. **A**, 159 (2000).
  - [7] Spin Muon Collaboration (D. Adams *et al.* ) Phys. Rev. **D56**, 5330 (1997).
  - [8] R. L. Jaffe, Phys. Lett. **B313**, 131 (1992).
  - [9] Review of Particle Properties, C. Caso *et al.*, Eur. Phys. J. **C3** (1998).
  - [10] M. Kirchbach and L. Tiator, Nucl. Phys. **A604**, 385 (1996).
  - [11] V. De Alfaro, S. Fubini, G. Furlan, and C. Rossetti, *Currents in Hadron Physics* (Amsterdam: North Holland, 1973 ).  
R. K. Bhaduri, *Models of the Nucleon* (California, Addison-Wesley, 1988).
  - [12] S. A. Coon and M. D. Scadron, Phys. Rev. **C42**, 2256 (1990).
  - [13] B. Machet, Int. J. Mod. Phys. **A14**, 4003 (1990).
  - [14] B. Krusche *et al.*, Phys. Rev. Lett. **74**, 3736 (1995);  
L. Tiator, C. Bennhold, and S. Kamalov, Nucl. Phys. **A580**, 455 (1994).
  - [15] A. Reuber, K. Holinde, and J. Speth, Nucl. Phys. **A570**, 541 (1991).
  - [16] G. Ecker, J. Gasser, A. Pich, and E. de Rafael, Nucl. Phys. **B321**, 311 (1989).
  - [17] R. Machleidt, Adv. Nucl. Phys. **19**, 189 (1989).
  - [18] R. Machleidt, K. Holinde, and C. Elster, Phys. Rep. **149**, 1 (1987).
  - [19] W. Grein and P. Kroll, Nucl. Phys. **A338**, 332 (1980).
  - [20] F. Gross, J. W. Van Orden, and K. Holinde, Phys. Rev. **C41**, R1909 (1990).
  - [21] T. Bolton *et al.*, Phys. Lett. **B279** 495 (1992).
  - [22] Bing-song ZOU, [hep-ph/9611238](#)
  - [23] A. Reuber, K. Holinde, H. C. Kim, and J. Speth, Nucl. Phys. **A608**, 243 (1996).
  - [24] V. I. Ogievetsky and B. M. Zupnik, Nucl. Phys. **B24**, 612 (1970).
  - [25] S. Neumeier, Diploma Thesis, TH Darmstadt, Germany, 1996, unpublished.
  - [26] T. Mizutani, C. Fayard, G.-H. Lamot, and B. Saghai, Phys. Rev. **C58**, 1551 (1998).

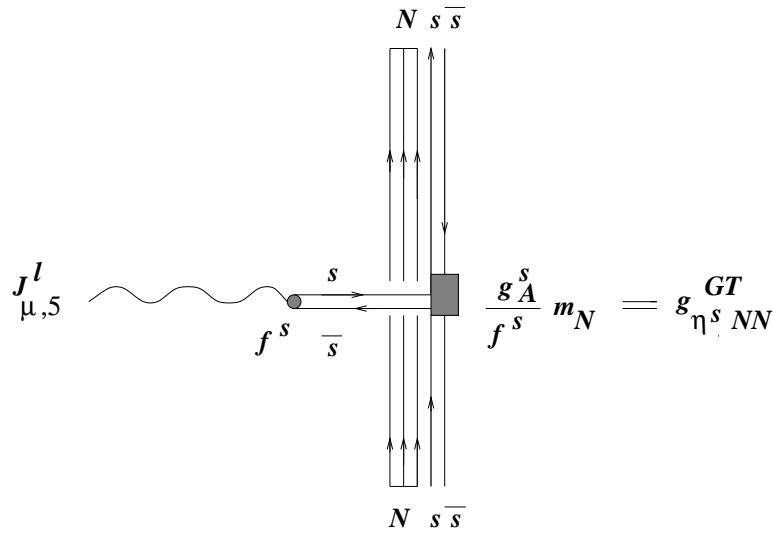


Fig. 1 Universality of the strange axial quark current and Goldberger-Treiman  $\bar{s}sN$  coupling.

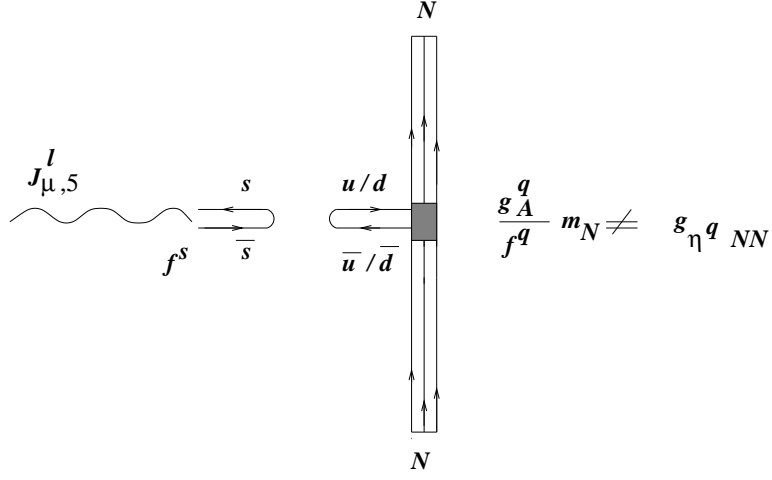


Fig. 2 Violation of current universality by the non-strange isosinglet axial current.

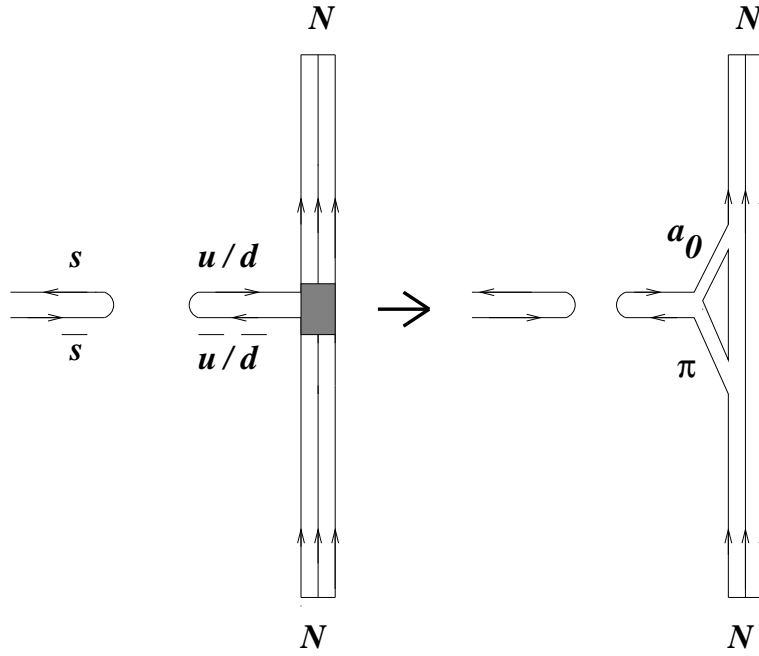


Fig. 3 Coupling isosinglet  $0^-$  non-strange quarkonium to the nucleon via triangular loops.

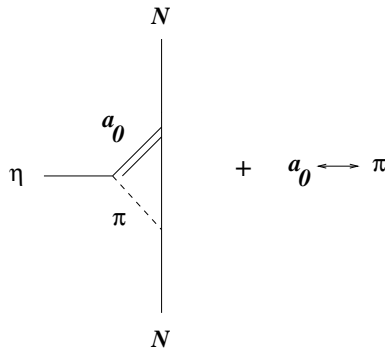
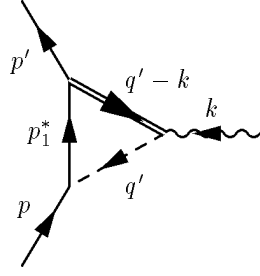
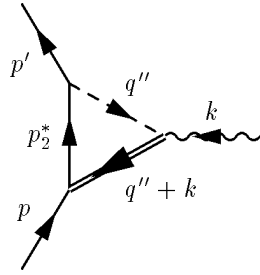


Fig. 4 The triangular  $\eta NN$  vertex.



a



b

Fig. 5 The flow of momentum.

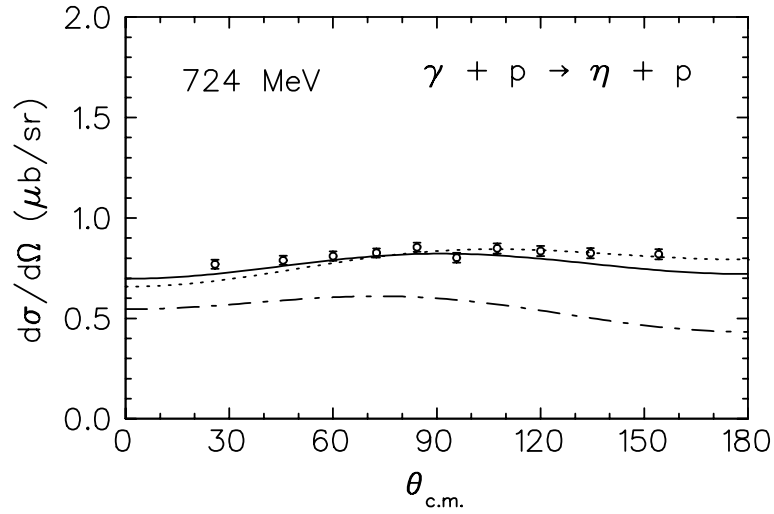


Fig. 6 Differential cross section for  $\eta$  photo-production off proton at lab energy of 724 MeV as calculated within the model of Tiator, Bennhold and Kamalov [14]. The dotted and dash-dotted lines correspond to  $g^2_{\eta NN}/4\pi$  taking the values of 0.4 and 1.1, respectively. The full line corresponds to the re-examined  $a_0\pi N$  triangular coupling with  $g^2_{a_0 NN}/4\pi \approx 6.79$ . The data are taken from Krusche et al. [14].

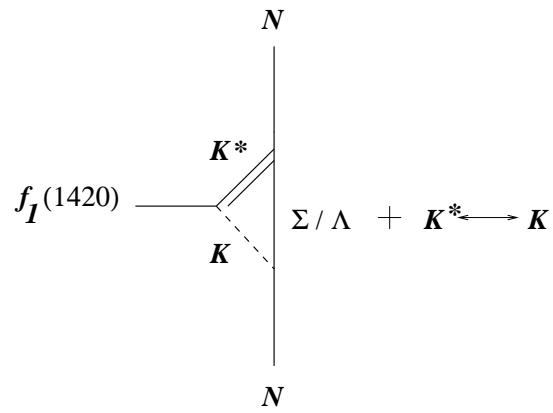


Fig. 7 The triangular  $f_1(1420)NN$  vertex.